Temperature dependence of the organization and molecular interactions within phospholipid/diacetylene Langmuir films

F. Gaboriaud [a,b,1], R. Volinsky [a,b], A. Berman [a,c], R. Jelinek [a,b,*]

[a] *Ilse Katz Center for Nano- and Meso-Science and Technology, and Department of Chemistry and Department of Biotechnology Engineering, Ben Gurion University, Beersheva 84105, Israel*
[b] *Chemistry Department, Ben Gurion University, Beersheva 84105, Israel*
[c] *Department of Biotechnology Engineering, Ben Gurion University, Beersheva 84105, Israel*

Abstract

Surface pressure–area isotherms and Brewster angle microscopy images of mixed binary films of dimyristoylphosphatidylcholine (DMPC) and the diacetylene 10,12-tricosadiynoic acid (TRCDA) were recorded at different temperatures and mole ratios to investigate the molecular interactions and cooperative properties of the films. The experiments revealed that segregation, on the one hand, and significant intermolecular interactions, on the other hand, both contribute to the thermodynamic properties of the phospholipids and the diacetylene assemblies. In particular, the data demonstrate that higher temperatures and greater percentage of DMPC promote repulsion between the liquid-condensed phospholipid monolayer and the TRCDA domains. In contrast, at high TRCDA mole ratios, film contraction occurred (lower molecular areas) due to TRCDA multilayer formation (at high temperature) or intermolecular affinities (at low temperature).
© 2005 Elsevier Inc. All rights reserved.

Keywords: Langmuir films; Polydiacetylene; Phospholipid films; Brewster angle microscopy

1. Introduction

Deciphering the organization and interactions of multi-component Langmuir films is an active field of research [1–5]. The interactions and organization of two molecular components occupying the same two-dimensional space have been explored by thermodynamic [6,7] and microscopic [2,8–10] approaches. Monolayers component miscibility [6], distribution [11] domain growth [12], nucleation [13], phase transition [14], and collapse [15] processes have attracted great interest ever since the early pioneering studies of Langmuir films [16,17]. Elucidating the association and cooperative phenomena of *lipids* and their interactions with other components in film environments is particularly important because of the significance of lipid assemblies in biological systems, specifically cellular membranes [18].

The aim of this study was to investigate the association properties and intermolecular interactions within films of dimyristoylphosphatidylcholine (DMPC), a phospholipid abundant in biological membranes, and 10,12-tricosadiynoic acid (TRCDA), a lipid diacetylenic molecule that has attracted significant interest because of the unique chromatic properties of its conjugated (polymerized) phase. Mixed films of DMPC and TRCDA have been previously investigated using varied spectroscopic, microscopic, and surface-analysis techniques [19,20]. Here we compare the thermodynamic properties of mixed DMPC/TRCDA films in different compositions and at three temperatures. Surface pressure–area isotherm analysis and Brewster angle microscopy (BAM) [21–24]. Illuminated the effects of temperature and film composition upon the intermolecular interactions and organization of the film components.

* Corresponding author. Fax: +972-8-6472943.
E-mail address: razj@bgu.ac.il (R. Jelinek).
[1] Present address: Laboratoire de Chimie Physique et Microbiologie pour l'Environnement, UMR 7564 CNRS-UHP Nancy 1, 405 rue de Vandoeuvre, 54600 Villers-lès-Nancy, France.

2. Experimental

2.1. Materials

TRCDA was purchased from GFS Chemicals (Powell, OH). The compound was purified by dissolving the solid in chloroform ($CHCl_3$) and the resulting solution filtrated in a 0.45-μm nylon filter. The purified solid was obtained by evaporation of the solvent. DMPC (Avanti Polar Lipids, Alabaster, AL) was used as received. The DMPC and TRCDA were dissolved in chloroform at a concentration of 2 mM. The various molar fractions were prepared by mixing the appropriate amounts of parent solutions of each compound. The water subphase used in the Langmuir trough was doubly purified by a Barnstead D7382 water purification system (Barnstead Thermolyne Corporation, Dubuque, IA-USA), with 18.3 mΩ resistivity.

2.2. Surface pressure–area isotherms

All surface pressure–area isotherms were measured with a computerized Langmuir trough manufactured by NIMA (Model 622/D1, Nima Technology Ltd., Coventry, UK). The experiments were carried out at different temperatures using a thermostated Teflon barostat (7×50 cm^2). The surface pressure was monitored using a 1-cm-wide filter paper as a Wilhelmy plate. For each isotherm experiment, 25 μL of the phospholipid/TRCDA solution in chloroform (2 mM) was spread on the water subphase (pH 6.3). To allow evaporation of solvent, the compression was started 15 min after spreading, using a constant barrier speed of 3.3 Å^2 molecule^{-1} min^{-1}. The surface pressure measurements were repeated at least three times, using a fresh mixture in each experiment. The isotherms presented are the average of three experimental runs (three surface pressure values per each molecular area), which were reproducible within the error area of ± 0.6 Å^2 molecule^{-1}.

2.3. Brewster angle microscopy

An NFT (Gottingen, Germany) Brewster angle microscope (BAM) mounted on a Langmuir film balance was used to observe the microscopic structures in situ. The light source of the BAM was a frequency-doubled Nd:YAG laser with a wavelength of 532 nm and primary output power 20–70 mW in a collimated beam. The BAM images were recorded with a CCD camera. The scanner objective was a Nikon superlong working distance objective with a nominal $10\times$ magnification and diffraction-limited lateral resolution of 2 μm. The images were corrected to eliminate side ratio distortion originating from a nonperpendicular line of vision of the microscope.
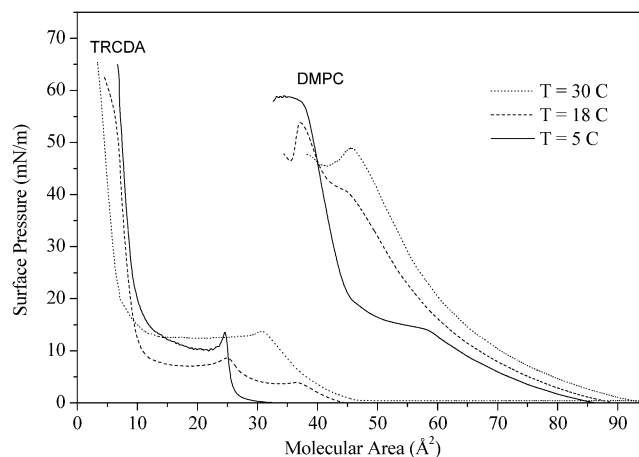

Fig. 1. Surface pressure–area isotherms of pure TRCDA and pure DMPC at 5, 18, and 30 °C.

3. Results and discussion

We explored the molecular properties of the DMPC/TRCDA films by analysis of the surface pressure–area (π–A) isotherms at 5, 18, and 30 °C. Initially, we recorded the pressure–area isotherms of pure films of TRCDA and DMPC at the three temperatures (Fig. 1). The isotherms exhibit significantly different compression profiles due to the distinct structural features of DMPC and TRCDA, respectively. Specifically, the two alkyl chains and bulky phosphatidylcholine headgroup of DMPC gave rise to much higher molecular areas in the entire temperature range ($A > 40$ Å^2 molecule^{-1}) compared to TRCDA, which has a smaller carboxylic headgroup and only a single alkyl residue.

Different thermal effects on the pure DMPC and TRCDA films are apparent in Fig. 1. At 30 °C, the isotherm of DMPC exhibits an expanded phase at a wide range of surface pressures, collapsing at around 50 mN m^{-1} with a limiting molecular area of 67 Å^2 molecule^{-1}. The high value of limiting molecular area and the relatively high stability of the expanded phase at this temperature is characteristic of the two alkyl-chain structure of phospholipids [25–27]. However, the expanded phase appeared less stable at 18 and 5 °C which featured phase transitions at around 40 and 15 mN m^{-1}, respectively [28–30]. This transition corresponds to the formation of a more organized condensed monolayer phase stabilized by the lower thermal motion of the phospholipid alkyl chains. The lower surface pressure in which this transition occurred as the temperature is reduced (40 mN m^{-1} at 18 °C compared to 14 mN m^{-1} at 5 °C) is explained by the slower molecular motion that facilitates closer interactions between the film components.

The thermodynamic features observed for pure TRCDA films are different than DMPC (Fig. 1). In particular, the surface pressure–area isotherms of TRCDA are strongly affected by the propensity of the single-alkyl-chain diacetylene molecules to organize in multilayer films [19,20]. At

low surface pressures and low temperatures (5 °C), only a condensed phase with a limiting area of 26 Å^2 molecule^{-1} was observed, which collapsed around 13 mN m^{-1}. This condensed phase was also observed at 18 °C, but was preceded by an expanded phase forming at a surface pressure of 5 mN m^{-1}. The condensed monolayer phase, however, was not formed at 30 °C. At this relatively high temperature the expanded phase was stable up to 14 mN m^{-1}. At all three temperatures examined, further compression of the TRCDA films resulted in formation of trilayered structures with limiting molecular areas close to 10 Å^2 molecule^{-1} [19,20].

The influence of temperature on the surface pressure–area isotherms is generally related to the Brownian motion molecules in the films [31]. For example, the increase of the surface pressure of the phase transition between expanded phase and condensed phase at higher temperatures, observed for both DMPC and TRCDA, is attributed to the higher Brownian motion which stabilizes the expanded phase. Essentially, the invested energy required to maintain molecules in a condensed monolayer phase (i.e., the surface pressure on the Langmuir trough) increases with the temperature [3,32,33].

While temperature and Brownian motion effects have been extensively studied for films of pure compounds, much fewer reports exist in the literature concerning the influence of temperature on isotherms of mixed Langmuir films. The thermodynamic analyses of films having different TRCDA:DMPC ratios at 5, 18, and 30 °C, respectively, reveals distinct differences in the appearances of the surface pressure/area isotherms (Fig. 2). A common feature of the films at all three temperatures is the difference between films containing higher fractions of DMPC ($X_{DMPC} \geqslant 0.5$) and films with higher ratios of TRCDA. Specifically, in films containing more DMPC the dominant features in almost the entire pressure range were the expanded monolayer phase formed by the DMPC molecules [20]. In addition, the collapse of the films with higher DMPC ratios occurred at different surface pressures. In contrast, when less DMPC than TRCDA molecules were incorporated in the mixed films ($X_{DMPC} \leqslant 0.5$), the isotherms generally exhibited at least one phase transition, and the collapse pressures were almost constant—around 53, 51 and 50 mN m^{-1} at 5, 18, and 30 °C, respectively.

Analysis of the isotherms of the mixed films is aided by application of the phase rule, which examines in this work the relationship between the surface pressures and the molecular areas at the phase transitions. Specifically, for a two-component monolayer, the number of degrees of freedom at the interface between the two molecular species corresponds to $F = 3 - q$, where q is the number of surface phases at equilibrium with each other [31,34–36]. This simple equation essentially indicates that in case of two *miscible* components, two homogeneous phases will be present in equilibrium at a phase transition. Thus, in this situation the system would possesses <u>one</u> degree of freedom, implying a first-order relation between the transition pressure and
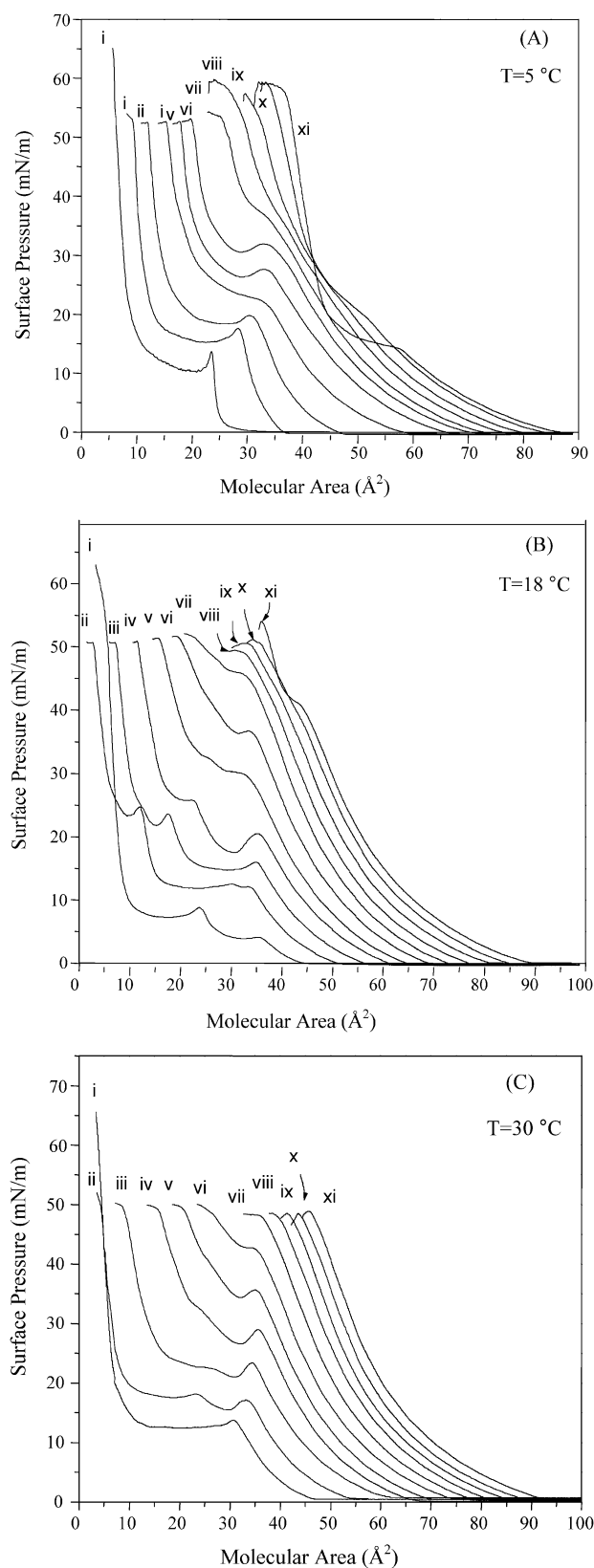

Fig. 2. Surface pressure–area isotherms of DMPC/TRCDA films, containing different mole fractions of DMPC, spread on a pure water subphase at (A) 5, (B) 18, and (C) 30 °C. The molar fractions of DMPC in the films were (i) 0 [pure TRCDA]; (ii) 0.1; (iii) 0.2; (iv) 0.3; (v) 0.4; (vi) 0.5; (vii) 0.6; (viii) 0.7; (ix) 0.8; (x) 0.9; (xi) 1.0 [pure DMPC].

film composition. Conversely, if the two components are *immiscible*, then three surface phases will coexist at the phase transition—meaning <u>zero</u> degrees of freedom, for example, a constant surface pressure during the phase transition.

Application of the phase rule provides insight into the organization of the films at the different temperatures and mole ratios. Examination of the surface pressure of the phase transition recorded for the mixed films at 5 °C reveals a clear variability at DMPC mole ratios lower than 0.6 (Fig. 2A). For example, at $X_{(DMPC)} = 0.5$ (curve vi in Fig. 2A), the transition occurred at a surface pressure of approximately 33 mN m^{-1}, while at $X_{(DMPC)} = 0.1$ (curve ii in Fig. 2A), the transition pressure was 17 mN m^{-1}. The variation in this particular phase transition (ascribed to the transformation of the TRCDA from a condensed monolayer into a trilayer) indicates that DMPC and TRCDA are miscible at 5 °C in this composition range and surface pressures. However, the constant film collapse at around 53 mN m^{-1} in these compositions clearly points to immiscibility of DMPC and TRCDA in this high surface pressure.

Different monolayer behavior was observed in films containing DMPC mole fractions higher than 0.6 at 5 °C (curves viii–x in Fig. 2A). In these compositions, the isotherms feature just a single phase corresponding to the condensed DMPC monolayer. In addition, the monolayers collapsed at markedly different surface pressures (for each composition), indicating the existence of miscibility between the two components. Importantly, TRCDA still induced significant effects on film behavior even at low concentrations; the expanded phase/condensed phase transition observed at 60 Å^2 molecule^{-1}, 15 mN m^{-1} in the pure DMPC monolayer (curve xi in Fig. 2A) essentially disappeared when just 10% TRCDA was incorporated within the film (curve x in Fig. 2A).

Single-phase organization was also apparent at 18 and 30 °C in films containing high fractions of DMPC (curves vii–x in Figs. 2B and 2C, respectively). Miscibility of DMPC and TRCDA at 18 °C was deduced from the progressive increase in collapse pressures in films containing high DMPC:TRCDA ratios (curves viii–x in Fig. 2B). However, when the mixed films at 18 °C incorporated higher percentages of the TRCDA, the two components became immiscible. This interpretation arises from both the similar surface pressures of the phase transition between the two condensed phases of the TRCDA film at around 25 mN m^{-1} (curves ii–iv in Fig. 2B), and from the almost uniform collapse pressure at approximately 51 mN m^{-1} when the TRCDA mole fraction was above 0.5 (curves ii–vi, Fig. 2B).

The thermodynamic profiles of the DMPC/TRCDA films at 30 °C (Fig. 2C) showed the clearest and most striking transformation between miscibility and immiscibility, occurring at equimolar concentrations of the components. The isotherms of films with ratios of DMPC:TRCDA higher than 0.5 featured a single expanded phase. The collapse pressures of these films were surprisingly constant (curves vii–x, Fig. 2C) indicating immiscibility between DMPC and

TRCDA (see discussion above). However, when the mole fraction of DMPC in the mixed films was lower (curves ii–vi, Fig. 2C), the transition at around 35 Å^2 molecule^{-1} between the low-surface-pressure expanded phase and the more condensed phase was clearly dependent upon the molar fractions. The increase in surface pressure of this transition, from around 13 mN m^{-1} (curve ii in Fig. 2C) to more than 40 mN m^{-1} (curve vi in Fig. 2C), points to the miscibility of the DMPC and TRCDA components in these film compositions.

Further insights into the interactions between the phospholipid and diacetylene constituents in the binary films were obtained through application of the additivity rule [36]
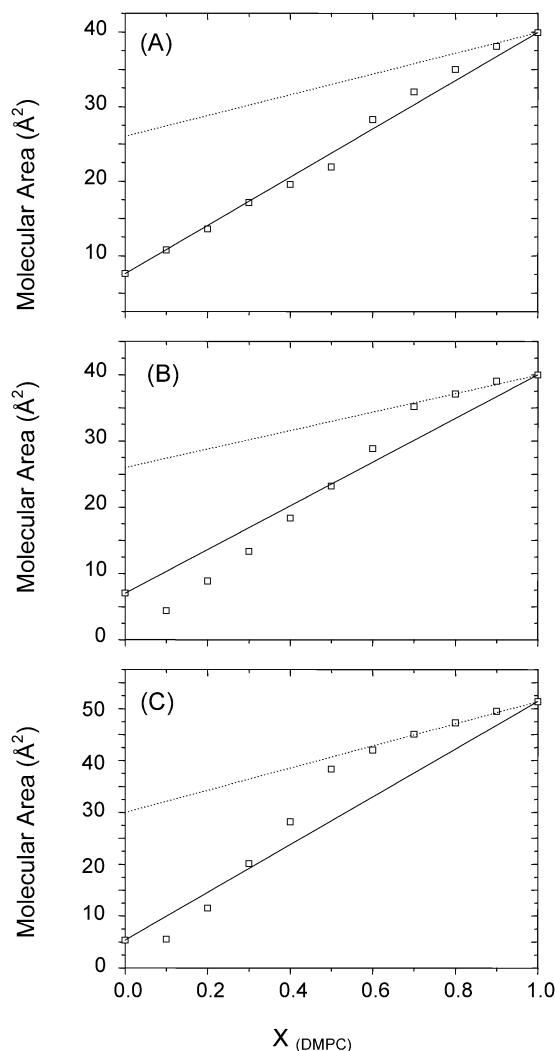

Fig. 3. Average molecular area of mixed DMPC/TRCDA films as a function of the molar fraction of DMPC, measured at a surface pressure of 47.5 mN m^{-1}: (A) 5, (B) 18, and (C) 30 °C. The solid and dotted lines represent the molecular areas determined by a statistical distribution of the TRCDA and DMPC components and are calculated according to the additivity rule: (A) TRCDA trilayer and DMPC condensed monolayer; (B) TRCDA trilayer and DMPC condensed monolayer (solid line), and TRCDA monolayer and DMPC condensed monolayer (dotted line); (C) TRCDA trilayer and DMPC expanded monolayer (solid line), and TRCDA monolayer and DMPC expanded monolayer (dotted line).
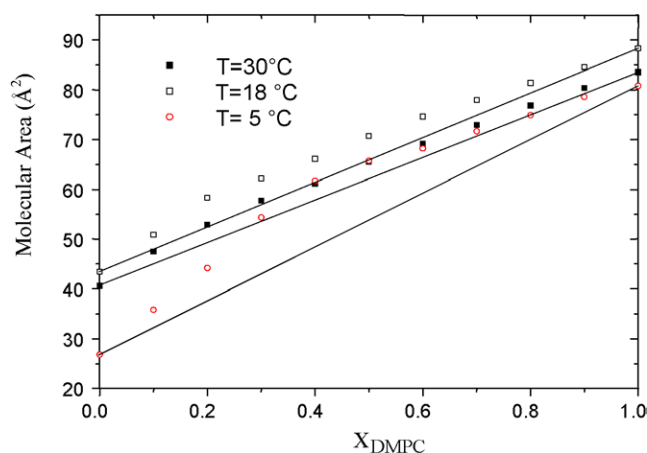
Fig. 4. Average molecular area of mixed DMPC/TRCDA films as a function of the molar fraction of DMPC, measured at a surface pressure of $1.5 \, \mathrm{mN\,m^{-1}}$. The straight lines correspond to statistical mixtures containing TRCDA and DMPC monolayers: long dash, 5 °C; solid line, 18 °C; short dash, 30 °C.

(Figs. 3 and 4). The additivity rule as applied in this study calculates the average molecular area ($\hat{A}_{\mathrm{mean}}$) at a given surface pressure by assuming an ideal binary mixture of *noninteracting* species. Specifically,

$$\hat{A}_{\mathrm{mean}} = (1 - X_{\mathrm{DMPC}}) A_{\mathrm{TRCDA}} + X_{\mathrm{DMPC}} A_{\mathrm{DMPC}},$$

where X_{DMPC} is the DMPC mole fraction in the film, A_{TRCDA} is the molecular area in a pure TRCDA film, and A_{DMPC} is similarly the molecular area of a pure DMPC monolayer. This calculation assumes an ideal mixture of noninteracting DMPC and TRCDA domains, with each domain adopting the organization and surface pressure of the pure constituent. Fig. 3 depicts graphs correlating the molecular areas recorded in each isotherm at a surface pressure of $47.5 \, \mathrm{mN\,m^{-1}}$ with the mole fraction of DMPC. The endpoints at the three graphs (i.e., at $X_{\mathrm{DMPC}} = 0$ and $= 1$) correspond to the molecular areas of *pure* trilayer TRCDA films and condensed monolayer DMPC films, respectively, at 5 and 18 °C (Figs. 3A, 3B) and of a TRCDA trilayer and an expanded DMPC monolayer at 30 °C (Fig. 3C). In that regard, the straight lines connecting the endpoints are essentially the molecular areas calculated at each fraction according to the additivity rule (i.e., "ideal" mixtures).

Comparison of the molecular areas recorded in the actual isotherms (squares in Fig. 3) with the data expected according to the additivity rule (straight lines) provides important information on the extent of intermolecular interactions within the films. At 5 °C almost all the experimental data points appear very close to the straight line corresponding to a pure statistical distribution of molecular components (Fig. 3A). This result indicates that the assumption of ideal mixtures comprising immiscible DMPC monolayers and TRCDA trilayers at 5 °C is indeed a valid description. The statistical mixture seems particularly pertinent for DMPC molar fractions lower than 0.5. A slight positive deviation from the straight line is observed at 5 °C in films with higher DMPC fractions (Fig. 3A, $X > 0.5$) suggesting that the TRCDA molecules might not adopt trilayer structures in these composition but are rather interspersed with the DMPC molecules in the monolayer.

In contrast to the data acquired at 5 °C (Fig. 3A), significant divergence of the experimental data from statistical mixtures were observed both at 18 °C (Fig. 3B) and at 30 °C (Fig. 3C). Two types of deviations were detected: positive (recorded molecular areas *above* the straight line corresponding to the additivity rule) and negative deviations (molecular areas below the line). Higher values of the molecular area (i.e., positive deviations) occurring for $X_{\mathrm{DMPC}} > 0.5$ (18 °C) and $X_{\mathrm{DMPC}} > 0.3$ (30 °C) indicate that the TRCDA trilayer used in the calculation does not accurately represent the real TRCDA structure in these composition ranges. Similarly to the interpretation of the positive deviations discussed above for 5 °C, the positive deviations observed in Figs. 3B and 3C indicate that the TRCDA molecules most likely organize in an expanded phase rather than a trilayer structure. Such an organization is expected to lead to pronounced repulsions between the film-incorporated film components. Such repulsions were clearly promoted by higher temperatures and higher DMPC fractions (Fig. 3), which is consistent with a higher mobility of the bulky DMPC molecules. Moreover, the positive divergence suggests that the incorporation of even small quantities of TRCDA into the DMPC films still induced a pronounced repulsion within the monolayers. Indeed, when applying the additivity rule with the TRCDA in a *monolayer* phase ($\sim 30 \, \mathrm{Å^2}$) rather than a *trilayer* (dotted lines in Figs. 3B and 3C), the experimental data points at high DMPC fractions completely coincide with the straight lines. This result is consistent with the miscibility of the two components in an expanded monolayer films.

Figs. 3B and 3C additionally point to the occurrence of *negative* deviations from ideal mixtures in films containing high TRCDA:DMPC ratios (more than 50% TRCDA at 18 °C, and more than 70% TRCDA at 30 °C). Such negative deviations most likely indicate that in these film compositions TRCDA forms multilayers rather than trilayers. This phenomenon was previously traced to the propensity of TRCDA to form multilayered structures in mixed films compressed at high surface pressures [19,20]. This interpretation is further reinforced by the transition at around $25 \, \mathrm{mN\,m^{-1}}$ at 18 °C (Fig. 2B, curves ii–iv), which was ascribed to a trilayer–multilayer transformation.

Interestingly, deviations of the recorded molecular areas compared to ideal mixtures were also apparent at *low* surface pressures (Fig. 4). Fig. 4 depicts the molecular areas recorded in the isotherms at the three temperatures at a surface pressure of $1.5 \, \mathrm{mN\,m^{-1}}$. In this low pressure both TRCDA and DMPC exist in a condensed (at 5 °C) or expanded (at 18 and 30 °C) monolayers. However, the positive deviations occurring within all film composition clearly indicate that significant intermolecular interactions occur even at this low pressure. Specifically, the positive devia-
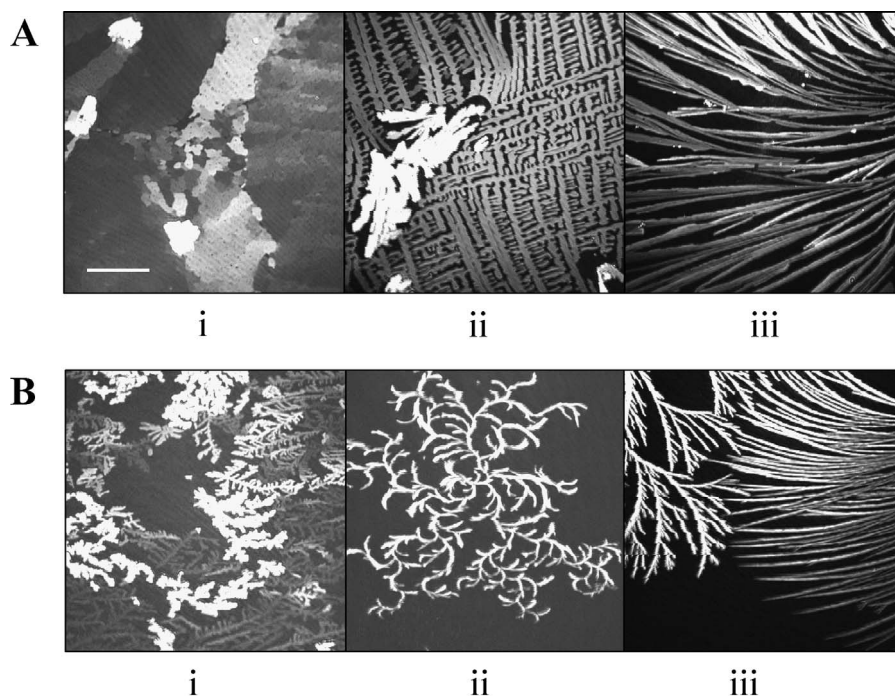
Fig. 5. BAM images of (A) pure TRCDA film and (B) mixed TRCDA/DMPC film (4:1 mole ratio) recorded at the phase transition at three temperatures: (i) 5, (ii) 18, and (iii) 30 °C. The bar represents 100 μm.

tions of molecular areas could arise from electrostatic repulsion among the negatively charged TRCDA headgroups and/or TRCDA and phosphate residues within DMPC. Indeed, such intermolecular repulsion is expected to be a more pronounced at 5 °C (Fig. 4), which is consistent with more significant repulsion experienced by the less mobile molecules in the condensed monolayer at this temperature.

The BAM images in Fig. 5, taken in the monolayer–multilayer phase transition regions (plateau regions of the isotherms), illuminate the organization of the TRCDA domains in pure diacetylene (Fig. 5A) and in the mixed films (Fig. 5B). In pure TRCDA films, at 5 °C (Fig. 5Ai) the film exhibits both a condensed monolayer phase (the pale dense regions) and the multilayer's nucleation regions (bright spots), at 18 °C both phases coexisted at phase transition, but the monolayer domains featured a dendritic character (Fig. 5Aii) due to nonequilibrium growth at this temperature. At 30 °C (Fig. 5Aiii) no condensed TRCDA monolayer was observed because the higher temperature essentially stabilized the liquid expanded phase, which is invisible in the BAM analysis. Interestingly, the multilayer domains also exhibited structural changes, acquiring stripelike shapes that might arise from the direct transition from the liquid-expanded phase, avoiding the condensed phase formation.

A similar behavior was observed in case of the mixed DMPC/TRCDA films (Fig. 5B). For example, at 5 °C, films containing 20 mol% DMPC featured both the condensed monolayer phase (the pale dendritic regions) and the trilayer structures (bright domains) was observed (Fig. 5Bi). The existence of dendritic TRCDA structures at low temperature can be explained by the effect of phospholipids which stabilize the liquid-condensed phase of TRCDA [8]. At 18 °C (Fig. 5Bii), a two-dimensional TRCDA trilayer growth was observed. Furthermore, no condensed monolayer was observed, which is different than the pure TRCDA film (Fig. 5A). Elimination of the condensed monolayer could be ascribed to the presence of the phospholipids and the higher temperature. The long anisotropic domains observed at 30 °C (Fig. 5Biii) resemble those in pure TRCDA film. Overall, the BAM data in Fig. 5 indicates that increasing the temperature resulted in destabilization of the *condensed TRCDA monolayer*, inducing instead direct transitions from the expanded monolayer to the multilayer film organization.

4. Conclusions

This study investigated the organization and interactions of mixed Langmuir films of a phospholipid (DMPC) and diacetylene (TRCDA) through recording of surface pressure–area isotherms and BAM images of films of different compositions and at three temperatures. Careful analysis of the isotherms, combined with applications of the phase rule and the additivity rule exposed the interplay between miscibility and immiscibility of the two film components, and revealed the role of each molecule in shaping film properties. The data help shedding light on the distinct structural features of TRCDA and DMPC at each temperature and film composition and the mutual interactions between the film domains. BAM imaging provided vivid pictures of the different TRCDA domains and their dependence upon temperature

and film composition. Overall, the experiments presented here demonstrate that different and competing factors contribute to binary film organization, and could help elucidate the roles of different biological molecules in phospholipid assemblies, particularly biological membranes.

Acknowledgments

References

[1] S. Wang, J. Ramirez, Y. Chen, P.G. Wang, R.M. Leblanc, Langmuir 15 (1999) 5623.
[2] S. Wang, R. Lunn, M.P. Krafft, R.M. Leblanc, Langmuir 16 (2000) 2882.
[3] A.M. Goncalves da Silva, J.C. Guerreiro, N.G. Rodrigues, T.O. Rodrigues, Langmuir 12 (1996) 4442.
[4] E. Gyorvary, W.M. Albers, J. Peltonen, Langmuir 15 (1999) 2516.
[5] M. Kawaguchi, M. Yamamoto, T. Kato, Langmuir 13 (1997) 2414.
[6] D.J. Crisp, Surface Chemistry Suppl. Research, Butterworths, London, 1949.
[7] D.K. Schwartz, Surf. Sci. Rep. 27 (1997) 241.
[8] M. Amrein, A. von Nahmen, M. Sieber, Eur. Biophys. J. 26 (1997) 349.
[9] E. Teer, C.M. Knobler, C. Lautz, S. Wurlitzer, J. Kildae, T.M. Fischer, J. Chem. Phys. 106 (5) (1997) 1913.
[10] G. Zhang, Y. Kuwahara, J. Wu, M. Akai-Kasaya, A. Saito, M. Aono, Surf. Sci. 476 (2001) L254.
[11] V. Vie, N. Van Mau, E. Lesniewska, J.P. Goudonnet, F. Heitz, C. Le Grimellec, Langmuir 14 (1998) 4574.
[12] U. Gehlert, D. Vollhardt, Langmuir 13 (1997) 277.
[13] D. Vollhardt, Colloids Surf. A Physicochem. Eng. Aspects 143 (1998) 185.
[14] G.A. Overbeck, D. Honig, D. Mobius, Langmuir 9 (2) (1993) 555.
[15] J. Saccani, S. Castano, F. Beaurain, M. Laguerre, B. Desbat, Langmuir 20 (2004) 9190.
[16] I. Langmuir, Trans. Faraday Soc. 15 (1920) 62.
[17] I. Langmuir, J. Am. Chem. Soc. 39 (1917) 1848.
[18] L. Prescott, J.P. Harley, D.A. Klein, Microbiology, third ed., De Boeck & Larcier, Brussels, 1999.
[19] R. Volinsky, F. Gaboriaud, A. Berman, R. Jelinek, J. Phys. Chem. B 106 (2002) 9231.
[20] F. Gaboriaud, R. Golan, R. Volinsky, A. Berman, R. Jelinek, Langmuir 17 (2001) 3651.
[21] D. Vollhardt, Mater. Sci. Eng. C 22 (2002) 121.
[22] D. Honig, G.A. Overbeck, D. Mobius, Adv. Mater. 4 (6) (1992) 419.
[23] D. Honig, D. Mobius, J. Phys. Chem. 95 (12) (1991) 4590.
[24] S. Henon, J. Meunier, Rev. Sci. Instrum. 64 (4) (1991) 936.
[25] H. Burner, R. Benz, H. Gimmler, W. Hartung, W. Stillwell, Biochim. Biophys. Acta 1150 (1993) 165.
[26] D. Gorwin, G.T. Barnes, Langmuir 6 (1990) 222.
[27] M.A. Bos, T. Nylander, Langmuir 12 (1996) 2791.
[28] F. Caruso, F. Grieser, P.J. Thistlethwaite, M. Almgren, E. Wistus, E. Mukhtar, J. Phys. Chem. 97 (1993) 7364.
[29] I. Kubo, S. Adachi, H. Maeda, A. Seki, Thin Solid Films 393 (2001) 80.
[30] V. Rosilio, G. Albrecht, Y. Okumura, J. Sunamoto, A. Baszkin, Langmuir 12 (1996) 2544.
[31] M.C. Petty, Langmuir–Blodgett Films, Cambridge Univ. Press, Cambridge, UK, 1996.
[32] G. Baskar, A.B. Mandal, Langmuir 16 (2000) 3957.
[33] Y.S. Kang, D.K. Lee, Y.S. Kim, Synth. Met. 117 (2001) 165.
[34] K.S. Birdi, Self-Assembly Monolayer Structures of Lipids and Macromolecules at Interfaces, Kluwer Academic/Plenum, New York, 1999.
[35] R. Maget-Dana, Biochem. Biophys. Acta 1462 (1999) 109.
[36] G.L. Gaines Jr., Insoluble Monolayers at Liquid–Gas Interfaces, Wiley–Interscience, New York, 1966.